

Simulation of Heat Transfer Through Soil for the Investigation of Wildfire Impacts on  
Buried Utilities

by

Edward G. Richter

A Report

submitted to

Oregon State University

in partial fulfillment of  
the requirements for the  
degree of

Master of Science

Presented June 4, 2021

Commencement June 2021

## Table of Contents

Abstract .....	6
Introduction .....	7
Water Distribution System Contamination.....	9
Background .....	10
Modeling and Methodology .....	13
Heat Transfer Equations .....	13
Model Parameters .....	15
Results and Discussion.....	17
Heat Flux .....	18
Burn Duration, Thermal Diffusivity, and Surface Temperature.....	20
Heat transfer results at 0.1m below the surface .....	20
Heat transfer results at 0.3m below the surface .....	22
Heat transfer results at 0.46m below the surface .....	23
Depth Below Ground .....	24
Sensitivity Analysis.....	27
Fragility Function .....	29
Limitations .....	31
Conclusions and Future Work.....	32
Appendix .....	34

Heat transfer results at 0.2m below the surface .....	34
Heat transfer results at 0.4m below the surface .....	35
Heat transfer results at 0.5m below the surface .....	36
References .....	38

## List of Figures

<b>Figure 1.</b> Schematic of a typical water distribution system.....	8
<b>Figure 2.</b> Boundary condition schematic of conductive heat transfer through soil. ....	14
<b>Figure 3.</b> Soil temperature distribution (°C) for varying levels of constant surface heat flux with a thermal diffusivity of $1.8 \times 10^{-6} \text{ m}^2/\text{s}$ and thermal conductivity of $3.72 \text{ W/m } ^\circ\text{C}$ . (a) Heat flux of $15 \text{ kW/m}^2$ , (b) Heat flux of $20 \text{ kW/m}^2$ , (c) Heat flux of $25 \text{ kW/m}^2$ , and (d) Heat flux of $30 \text{ kW/m}^2$ .....	19
<b>Figure 4.</b> Soil temperature (°C) at 0.1m below the surface for a range of thermal diffusivities ( $0.5 \times 10^{-6} \leq \alpha \leq 1.8 \times 10^{-6} \text{ m}^2/\text{s}$ ) and constant surface temperatures (°C). (a) 15 minutes of burning, (b) 30 minutes of burning, (c) 1 hour of burning, (d) 2 hours of burning, and (e) 4 hours of burning.....	21
<b>Figure 5.</b> Soil temperature (°C) at 0.3m below the surface for a range of thermal diffusivities ( $0.5 \times 10^{-6} \leq \alpha \leq 1.8 \times 10^{-6} \text{ m}^2/\text{s}$ ) and constant surface temperatures (°C). (a) 1 hour of burning, (b) 2 hours of burning, and (c) 4 hours of burning.....	23
<b>Figure 6.</b> Soil temperature (°C) at 0.46m below the surface for a range of thermal diffusivities ( $0.5 \times 10^{-6} \leq \alpha \leq 1.8 \times 10^{-6} \text{ m}^2/\text{s}$ ) and constant surface temperatures (°C). (a) 2 hours of burning, and (b) 4 hours of burning.....	24
<b>Figure 7.</b> Soil temperature (°C) distribution to 0.5m below the surface with thermal diffusivity as ( $\alpha = 1.8 \times 10^{-6} \text{ m}^2/\text{s}$ ) for: (a) a representative structure fire ( $600^\circ\text{C}$ ), and (b) an upper bound structure fire ( $900^\circ\text{C}$ ).....	25

**Figure 8.** Soil temperature (°C) distribution to 0.5m below the surface with thermal diffusivity as ( $\alpha = 1.64 \times 10^{-6} \text{ m}^2/\text{s}$ ) for: (a) a representative structure fire (600°C), and (b) an upper bound structure fire (900°C) .....27

**Figure 9.** Tornado sensitivity plot of maximum and minimum soil parameters that contribute to below ground soil temperature that is representative of a WUI community. ....29

**Figure 10.** Fragility curve describing the probability of exceeding the maximum operational temperatures of buried pipes (60°C) based on burial depth (m). .....31

**Figure A-1.** Soil temperature (°C) at 0.2m below the surface for a range of thermal diffusivities ( $0.5 \times 10^{-6} \leq \alpha \leq 1.8 \times 10^{-6} \text{ m}^2/\text{s}$ ) and constant surface temperatures (°C). (a) 30 minutes of burning, (b) 1 hour of burning, (c) 2 hours of burning, and (d) 4 hours of burning .....35

**Figure A-2.** Soil temperature (°C) at 0.4m below the surface for a range of thermal diffusivities ( $0.5 \times 10^{-6} \leq \alpha \leq 1.8 \times 10^{-6} \text{ m}^2/\text{s}$ ) and constant surface temperatures (°C). (a) 2 hours of burning, and (b) 4 hours of burning .....36

**Figure A-3.** Soil temperature (°C) at 0.5m below the surface for a range of thermal diffusivities ( $0.5 \times 10^{-6} \leq \alpha \leq 1.8 \times 10^{-6} \text{ m}^2/\text{s}$ ) and constant surface temperatures (°C). (a) 2 hours of burning, and (b) 4 hours of burning .....37

## **Abstract**

Wildland urban interface (WUI) communities in the Western United States have recently dealt with historic and devastating wildfires year after year. The fires have cost tens of billions in damage, burned tens of thousands of structures, displaced thousands of residents, and killed over one hundred people. The 2017 Tubbs fire and 2018 Camp fire caused catastrophic infrastructure losses, and extensive fire damage to the water distribution systems in the towns of Santa Rosa and Paradise CA. Fire damage caused the water distribution system to become contaminated with volatile organic compounds (VOCs) including benzene, a well-known carcinogen. To this day the towns of Santa Rosa and Paradise are still recovering from the water contamination problems caused by the wildfires. This study investigates the heat transfer of wildfires through the soil to quantify if the maximum operational temperature (60°C) of common pipelines is exceeded during a wildfire. This was accomplished using a one-dimensional transient heat conduction model, that looks at the effect of burial depth, surface burn duration, surface temperature of the fire, surface heat flux, and the thermal diffusivity of the soil. Results of this research indicate that burial depths of pipelines and burn duration of the wildfire are key factors in determining if operational temperatures of the pipeline are exceeded. Under conditions that are expected in a wildfire affecting a WUI community in the intermountain West; maximum operational temperature of the pipelines was exceeded at depths up to 0.45m. A fragility analysis of burial depths reveals that operational temperature of the pipelines will be exceeded at least 50% of the time at depths up to 0.19m. This research will provide useful information for municipalities in WUI communities to plan for future resiliency against wildfires.

## Introduction

Wildfires have increased in frequency and intensity over the last 30 years, a trend that is especially problematic in wildland urban interface (WUI) communities. WUI communities are one of the fastest growing land use types in the United States (Radeloff et al. 2018). The 2017, 2018, and 2020 California fire seasons had particularly devastating impacts to WUI communities. The 2017 Tubbs Fire was, at the time of the fire, the most destructive and costliest wildfire on record. Although only 36,807 acres burned, 5,636 housing units were destroyed, with estimated losses costing \$9.4 billion at the time (Cal Fire 2020a; Kasler 2017). The record-breaking losses of the Tubbs Fire were soon surpassed by the 2018 Camp Fire. The Camp Fire was both the deadliest and costliest wildfire on record, where 85 people died and estimated losses were \$16.5 billion (Löw 2019). 153,336 acres burned destroying 11,300 housing units within the town of Paradise, and a total of 18,804 housing units were destroyed in the fire (Cal Fire 2018). The 2020 August Complex Fire was the first “Gigafire” burning over one million acres (Cal Fire 2020b).

One particularly devastating effect of both the Tubbs Fire and the Camp Fire was damage to and contamination of the water distribution system within the towns of Santa Rosa and Paradise. This contamination and damage lasted several months after the fire was over. Water testing is still occurring at the time of writing this report (Schulze et al. 2020). Volatile organic compounds (VOCs), including benzene, were discovered within the water distribution system shortly after the fire, prompting the Paradise Irrigation District to issue a city-wide water advisory (PID 2019). In an effort to determine the source of the contamination, Paradise Irrigation District began sampling various portions of the

water distribution system and replacing portions of pipe that were contaminated with VOCs.

A typical schematic of a water distribution system is shown in Figure 1, and is comprised of water mains, meter boxes, and service laterals. The water main is considerably larger in diameter (15.2 – 40.6 cm), buried at a larger distance from the ground surface 1.07m, and transports water throughout the system. Service lateral pipes are smaller in diameter (1.3 – 10.2 cm), located closer to the ground surface at a minimum of 0.305m, and serve as the primary distribution point into a structure (Duffy 2019). In addition, service lateral pipes connect a home or building to the water meter, and will be buried under wildfire fuel (e.g. brush, homes, trees) whereas water mains are typically buried under roadways where there is no fuel. Schulze and Fischer (2021) report that 3% of water main pipes tested in Paradise and Santa Rosa contained elevated levels of contaminants, while 19% of service lateral pipes tested had elevated levels of contaminants.

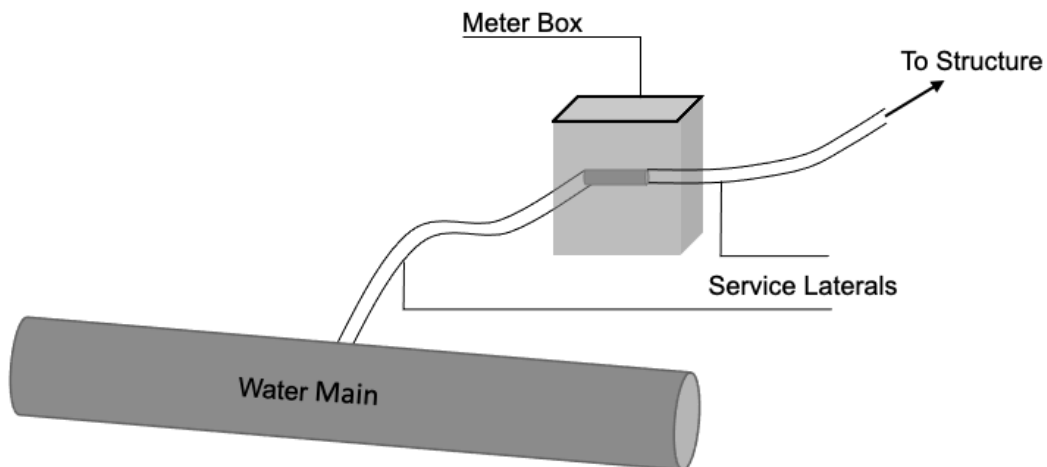


**Figure 1.** Schematic of a typical water distribution system.

## **Water Distribution System Contamination**

Two possible sources of contamination in the water distribution due to wildfires are 1) exposed service laterals that have been damaged during the fire (Santa Rosa 2018) and 2) thermal degradation of the service lateral pipes themselves (Chong et al. 2019; Isaacson et al. 2021).

Depressurization of the water system during a wildfire can cause an intake of toxic gasses from the burning environment (both built and natural) into the water distribution system. During a wildfire, damaged service laterals will continually leak water, causing extra demand on the water distribution system. Firefighting efforts during the wildfire produce additional demand on the water distribution system. All of the excess demand on the water distribution system can cause depressurization events throughout the system, which allows for toxic gases and ash to enter from nearby burning structures. The VOCs from the gasses and ash are then absorbed into the materials of the water distribution system (pipes, gaskets, etc.), and contaminants are slowly released back into the water within the system once normal water flow and pressure has been reestablished (Proctor et al. 2020). Backflow devices, when properly installed, can help prevent this. However, the town of Santa Rosa found that VOCs were still present in some of the service laterals in a few locations that had backflow devices installed (Schulze and Fischer 2021).

Another potential source of contamination is from the service lateral pipes themselves (Chong et al. 2019; Isaacson et al. 2021). Common service lateral pipe materials found throughout the United States include copper, galvanized steel, and

plastics, such as high-density polyethylene (HDPE), polyvinyl chloride (PVC), and cross-linked polyethylene (PEX). Historically, copper and steel pipes were used as pipe material for service laterals; however, in the later part of the 20<sup>th</sup> century plastic pipes have increased in popularity for both their affordability and ease of use during installation (Sharpe and Associates 2010). In the town of Paradise, copper and HDPE service laterals were the most common prior to the 2018 Camp Fire and experienced extensive damage during the wildfire (PID 2019).

These service lateral pipe materials are not tested at temperatures they are exposed to during a wildfire. Both Paradise and Santa Rosa found damaged service lateral pipes and both towns replaced all service laterals on private properties as a stipulation for receiving a certificate of occupancy for people to move back to their homes. Homes and buildings can burn for upwards of 4 hours depending on size and type, reaching peak temperatures of nearly 1000°C (Beitel and Iwankiw 2008; Schulze et al 2020).

## **Background**

The ability of heat to transfer down through soil has long been a focus in grasslands and forests (Massman et al. 2003; Wells et al. 1979), but is more recently coming into focus in WUI communities as a potential cause of damage to water distribution systems (Schulze and Fischer 2021). Degree of saturation, mineral content, organic matter, porosity, temperature, and grain size all contribute to and effect the thermal conductivity of soil (Ochsner et al. 2001; Smits et al. 2016; Campbell et al. 1994; Abu-Hamdeh 2003). For example, Abu-Hamdeh and Reeder (2000) found that thermal conductivity decreased

with increasing soil organic matter. As the degree of saturation of soil increases, soil thermal conductivity also increases (Smits et al. 2010). Soil temperature can also play a key role in the thermal conductivity of the soil where increased temperatures lead to increased levels of thermal conductivity (Campbell et al. 1994).

Another important and related soil parameter is thermal diffusivity ( $\alpha$ ). Thermal diffusivity is the rate of heat transfer in a solid from one temperature gradient to another. Thermal diffusivity and thermal conductivity ( $\lambda$ ) are intrinsically related by the simple relationship shown in Equation 1, where the thermal diffusivity ( $\alpha$ ) is the ratio of thermal conductivity ( $\lambda$ ) to the heat capacity of the soil ( $C$ ).

$$\alpha = \frac{\lambda}{C} \quad [1]$$

Scotter (1970) compared experimental data to a simplified mathematical model (Carslaw and Jaeger 1959) to calculate soil temperatures underneath a grass fire. The grass fire obtained a peak temperature of 300°C, and maintained temperatures of over 100°C for 80 seconds. Scotter (1970) measured elevated soil temperatures up to 4cm below the surface throughout this fire. When utilizing the mathematical model to calculate the soil temperatures, Scotter (1970) found that the calculated temperatures were highly correlated to the experimental data. Scotter (1970) also found that the duration the surface temperatures were over 100°C effected below ground soil temperatures more than the maximum temperature of the fire on the surface.

Grass fires have a shorter burn duration, decreased fuel loading, and lower peak temperatures when compared to wildfires in WUI communities (Rehm et al. 2002). Fuel

loading in an urban dwelling and office environment can be 40 – 100 times greater than what is found in grasslands, and 2 – 5 times greater than what is found in a heavy brush forest (Chandler et al. 1983). In WUI communities, housing density is a key factor that determines fuel loading, indicating that fuel loading will be variable within and between communities of different sizes and housing densities (Rehm et al. 2002). Research by Schulze and Fischer (2021), found that portions of WUI communities with increased housing density resulted in a higher probability of contaminants present in the water distribution system after a wildfire.

The objective of this research is to: (1) quantify the influence of thermal diffusivity, heating duration, surface temperature, and surface heat flux, on the thermal gradient through the soil and (2) calculate the probability that pipelines will exceed their operational temperature considering variation in thermal diffusivity, heating duration, surface temperature, and surface heat flux. This will be achieved by using mathematical models to solve transient heat conduction through a semi-infinite solid (Carslaw and Jaeger 1959) and developing a probabilistic fragility function to explore the influence of key parameters influencing thermal gradients through the soil. The results of this research will highlight the importance of testing pipelines at temperatures that exceed their operational temperature. This is to ensure that the pipe material is not contributing to contamination of the water within the water distribution system during a wildfire. Additionally, we aim to help inform future research into the wildfire impact of buried utilities in high-risk WUI communities.

## **Modeling and Methodology**

During a wildfire, heat transfers from burning entities (e.g. brush, homes, trees) to the surface of the soil via convection and radiation. However, heat transfer through a solid is controlled by conduction (Drysdale 2011). A simplifying assumption of conduction only heat transfer from wildfires was made for this report based on the work of (Scotter 1970). A further assumption of treating the ground as a semi-infinite solid is appropriate for the development of heat transfer models (Carslaw and Jaeger 1959). To calculate the temperature distribution through the soil under a home, a one-dimensional (1D) conductive heat transfer analysis was performed in Python.

### **Heat Transfer Equations**

The analysis presented within this paper is a transient 1D heat transfer analysis based on the partial differential equation shown in Equation 2. In this formulation,

$$\frac{\partial^2 T}{\partial x^2} = \frac{1}{\alpha} \frac{\partial T}{\partial t} \quad [2]$$

$\alpha$  is the thermal diffusivity of the soil,  $T$  is the surface temperature,  $x$  is the depth below ground, and  $t$  is time. To solve Equation 2, boundary conditions need to be defined (Figure 2). The first boundary condition,  $T(0, t)$  is temperature at  $t = 0$  on the surface of the ground,  $x = 0$ . In this study, the surface temperature will be defined in the analysis as a parameter to investigate. The second boundary condition defined, is the initial temperature of the soil,  $T_i$ , which is considered homogenous throughout the semi-infinite body, at  $t = 0$ .

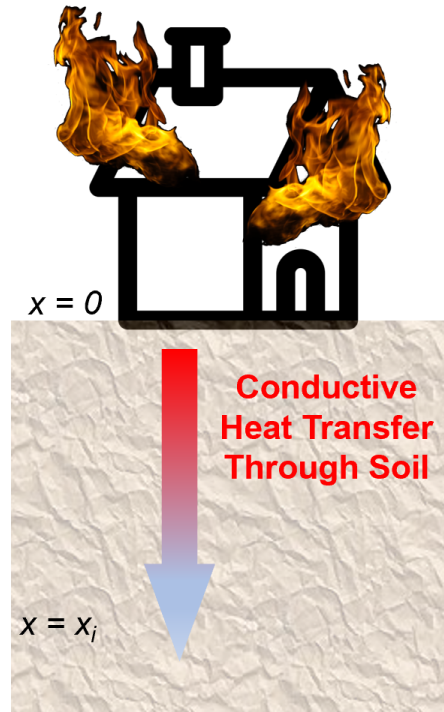


**Figure 2.** Boundary condition schematic of conductive heat transfer through soil.

Using the derivations performed by Carslaw and Jaeger (1959), when surface temperature is constant, Equation 2 can be simplified to Equation 3.

$$\frac{T(x, t) - T_i}{T_s - T_i} = \operatorname{erfc}\left(\frac{x}{2\sqrt{\alpha t}}\right) \quad [3]$$

The complementary error function,  $\operatorname{erfc}$ , is defined in Equation 4.

$$\operatorname{erfc}(\zeta) = 1 - \frac{2}{\sqrt{\pi}} \int_0^\zeta e^{-u^2} du \quad [4]$$

The complementary error function cannot be solved analytically, but numerical solutions have been solved. These values are commonly incorporated into computer programs such as the open-source math package in Python that have been used for the following analyses (Van Rossum 2020).

When the surface of a semi-infinite solid is exposed to a constant heat flux,  $\dot{Q}''$ , the temperature distribution through the solid can be calculated by solving the partial differential equation shown in Equation 5.

$$\frac{\partial^2 \dot{q}''}{\partial x^2} = \frac{1}{\alpha} \frac{\partial \dot{q}''}{\partial t} \quad [5]$$

Equation 5 is the same format as Equation 2; however, heat flux is considered the primary variable of the equation, instead of temperature. Solving Equation 5 with the boundary conditions of  $\dot{q}'' = \dot{Q}''$  at  $x = 0$  for all time greater than zero yields:

$$T(x, t) - T_i = \frac{\dot{q}''}{\lambda} \left[ \sqrt{\frac{4\alpha t}{\pi}} \exp\left(-\frac{x^2}{4\alpha t}\right) - x * \operatorname{erfc}\left(\frac{x}{2\sqrt{\alpha t}}\right) \right] \quad [6]$$

where  $T(x, t)$  is the temperature of the soil at a specific depth ( $x$ ) and time ( $t$ ). Through the algebraic manipulation of Equation 3, it is possible to determine the temperature in the soil based on depth ( $x$ ), surface temperature ( $T_s$ ), time ( $t$ ), and thermal diffusivity ( $\alpha$ ). Initial temperature of the soil ( $T_i$ ) was held at a constant 20°C as a representative average of the fluctuations in soil temperatures that occur daily and annually (Márquez et al. 2016).

### **Model Parameters**

Maximum operational temperatures of common service laterals are presented in Table 1. Copper and steel pipes have a much higher range of operating temperatures than plastic pipes, with HDPE and PVC having the lowest at 60°C. Typically, water distribution systems are designed for operation at 23°C. For temperatures that are expected to exceed 23°C reduction factors are introduced to account for the increased temperature

up to a specified maximum for the material (AWWA 2006). Industry recommended minimum burial depth for plastic pipes is 0.46m (MAB 2019), while the Uniform Plumbing Code (2021) requires a minimum of 0.305m below finished grade or 0.305m below the frost line for water piping installation.

A range of surface temperature values were selected not only based on conditions that would be commonly present during a fire, but also exploring the upper and lower bound potential surface temperatures. Service lateral burial depths up to 0.5m were considered to include the industry recommended burial depth of 0.46m within the bounds of the research investigation (MAB 2019).

**Table 1.** Common service lateral materials and corresponding maximum operational temperatures.

<b>Material</b>	<b>Maximum operational temperature (°C)</b>	<b>Source</b>	<b>ASTM</b>
PVC	60	Georg Fischer 2010	D1785
HDPE	60	PPI 2009	F2160
PEX	82	Home Innovations 2013	F876
Galvanized pipe	200	Duran 2013	A53
Copper Type K	204	CDA 2010	B88

Due to the high variability of factors that affect the thermal diffusivity of soils, a broad range of values representative of WUI communities were considered. This allows for the inclusion of different soil types and varying local conditions that could be present.

A thermal diffusivity range of  $0.5 \times 10^{-6} - 1.8 \times 10^{-6} \text{ m}^2/\text{s}$  was chosen based on previous research of soil types in WUI communities (Abu-Hamdeh 2003; Bilskie 1994; DeVries 1963; Márquez et al. 2016; Ochsner et al. 2001). For instances where a direct comparison is made to a WUI community, soil types were collected from the USDA Web Soil Survey tool (2019) and matched to thermal diffusivity values presented for specific soil types found in the literature.

Surface burn duration is dependent on available fuel for the fire. WUI communities have fuel loading that is estimated to be 40 – 100 times greater than a grassland (Chandler et al. 1983). Scotter (1970) found that surface temperatures in a grass fire remained elevated above  $100^\circ\text{C}$  for 80 seconds. Scaling that to a WUI wildfire would indicate sustained elevated temperatures for over two hours. A range of surface burn durations from 15-minutes to 4-hours were considered to include all possibilities that would be present in a WUI wildfire.

## **Results and Discussion**

The results of the 1D heat transfer analysis through the soil are presented in this section. First, general trends in how fire characteristics and soil properties influence the thermal gradient through the soil are summarized. Secondly, sensitivity and fragility analysis results are presented. These results highlight key parameters that influence the temperature profile through the depth of the soil during a wildfire.

## **Heat Flux**

Heat flux is the flow of energy per unit of time. Heat flux is often used to characterize fire intensity and will impact the surface temperature during a wildfire and the temperature gradient through the soil. Figure 3 shows the temperature distribution through the soil when the surface heat flux is varied, while the thermal diffusivity and thermal conductivity remain constant at  $1.8 \times 10^{-6} \text{ m}^2/\text{s}$  and  $3.72 \text{ W/m } ^\circ\text{C}$ , respectively. These values of thermal diffusivity and conductivity are representative of a sandy loam soil, which represent the upper range of what could be found in a WUI community (Ochsner et al. 2001). Each line represents a different burn duration of constant heat flux, showing that the soil temperature at various depths below the surface.

Figure 3a shows the soil temperature distribution ( $^\circ\text{C}$ ) when the surface heat flux remains constant at  $15 \text{ kW/m}^2$  for four different heating durations. This surface heat flux is representative of a low-intensity fire similar to the understory forest floor burning of pine needles (Silvani and Morandini 2009). Figure 3d shows the soil temperature distribution ( $^\circ\text{C}$ ) when the surface heat flux is set to  $30 \text{ kW/m}^2$  for the same four different heating durations. A surface heat flux of  $30 \text{ kW/m}^2$  is representative of a WUI fire with a house burning. Typical windows in a WUI community are designed for a heat flux of  $45 \text{ kW/m}^2$ , which could be the upper bound of a WUI fire (Kim and Lougheed 1990; Quarles and Sindelar 2011). Figures 3b and 3c use constant heat fluxes that fall in between a forest floor fire and a typical WUI fire.

The results presented in Figure 3 show that increasing the surface heat flux will increase the ground surface temperature during a fire. In Figure 3a, the surface

temperature for a two-hour fire with a constant surface heat flux of  $15 \text{ kW/m}^2$  is  $538^\circ\text{C}$  whereas in Figure 3d, the surface temperature for a two-hour fire with a constant surface heat flux of  $30 \text{ kW/m}^2$  is  $1056^\circ\text{C}$ . In addition, with increasing surface heat flux, the operational temperature of the pipe is exceeded at a shallower depth. In Figure 3a the operational temperature of the pipe was exceeded at  $0.24\text{m}$ , while in Figure 3d the operational temperature of the pipe was exceeded at  $0.28\text{m}$ .

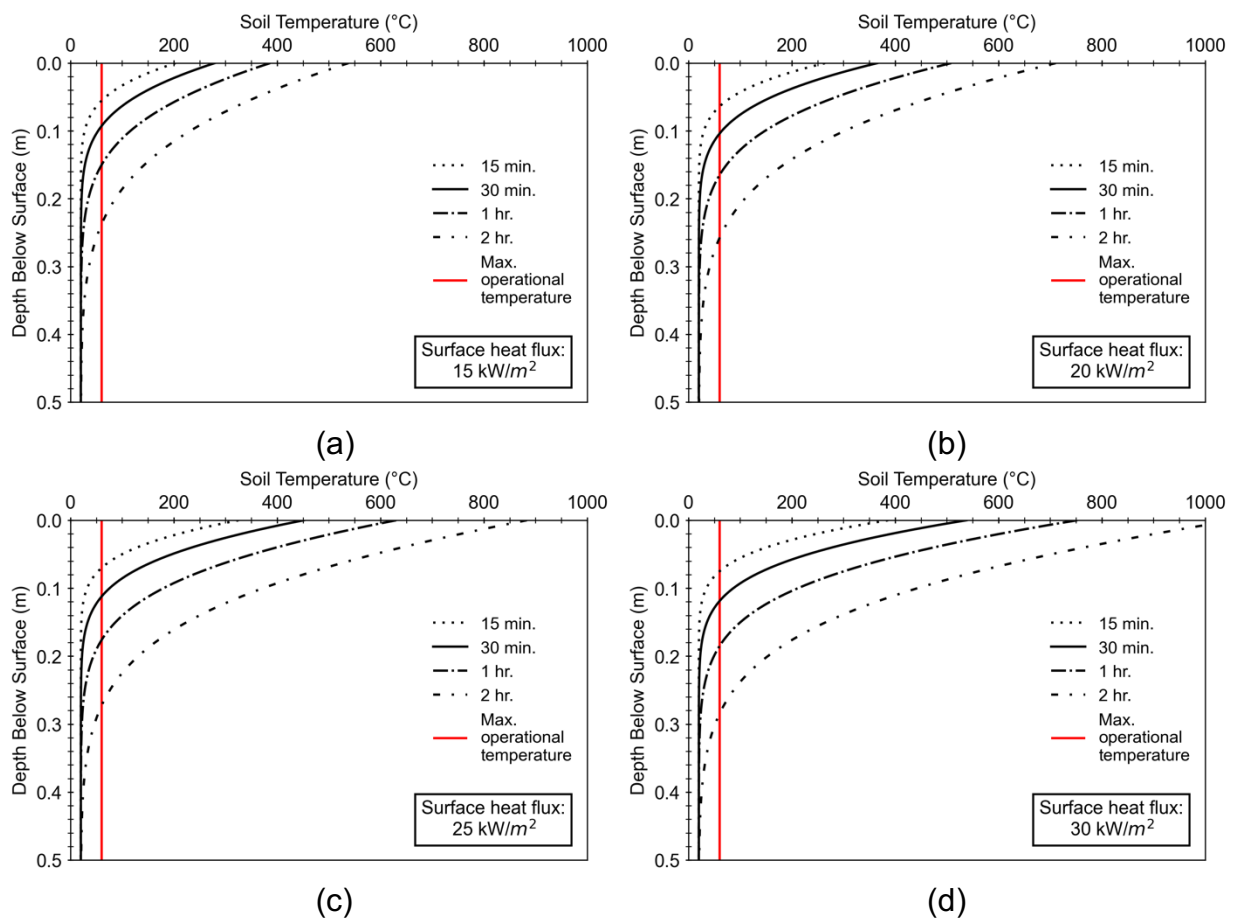


**Figure 3.** Soil temperature distribution ( $^\circ\text{C}$ ) for varying levels of constant surface heat flux with a thermal diffusivity of  $1.8 \times 10^{-6} \text{ m}^2/\text{s}$  and thermal conductivity of  $3.72 \text{ W/m } ^\circ\text{C}$ . (a) Heat flux of  $15 \text{ kW/m}^2$ , (b) Heat flux of  $20 \text{ kW/m}^2$ , (c) Heat flux of  $25 \text{ kW/m}^2$ , and (d) Heat flux of  $30 \text{ kW/m}^2$

## **Burn Duration, Thermal Diffusivity, and Surface Temperature**

Burn duration, thermal diffusivity, and surface temperature all influence the thermal distribution through the soil depth profile. Figures 4 – 6 show the results of the heat transfer analysis at 0.1m, 0.3m, and 0.46m below the surface of the ground for a range of burn durations, thermal diffusivity values, and surface temperatures. Analysis of additional depths of 0.2m, 0.4m, and 0.5m can be found in the Appendix at the end of this report.

### **Heat transfer results at 0.1m below the surface**

Operational temperatures of the pipes are exceeded at lower surface burn temperatures with increasing burn durations. Figure 4a shows that the maximum operational temperature of the pipes (60°C) is exceeded for a 15-minute burn duration once surface temperatures are in excess of 527°C with a thermal diffusivity of  $1.8 \times 10^{-6} \text{ m}^2/\text{s}$ . An increase in burn duration to 30-minutes is shown in Figure 4b, where maximum operational temperature of the pipes (60°C) is exceeded for surface temperatures above 207°C with a thermal diffusivity of  $1.8 \times 10^{-6} \text{ m}^2/\text{s}$ . The longest burn duration considered, 4-hours, (Figure 4e) shows that the maximum operational temperature of the pipes (60°C) is exceeded at surface burn temperatures of 81°C with a thermal diffusivity of  $1.8 \times 10^{-6} \text{ m}^2/\text{s}$  and at 119°C with a thermal diffusivity of  $0.5 \times 10^{-6} \text{ m}^2/\text{s}$ .

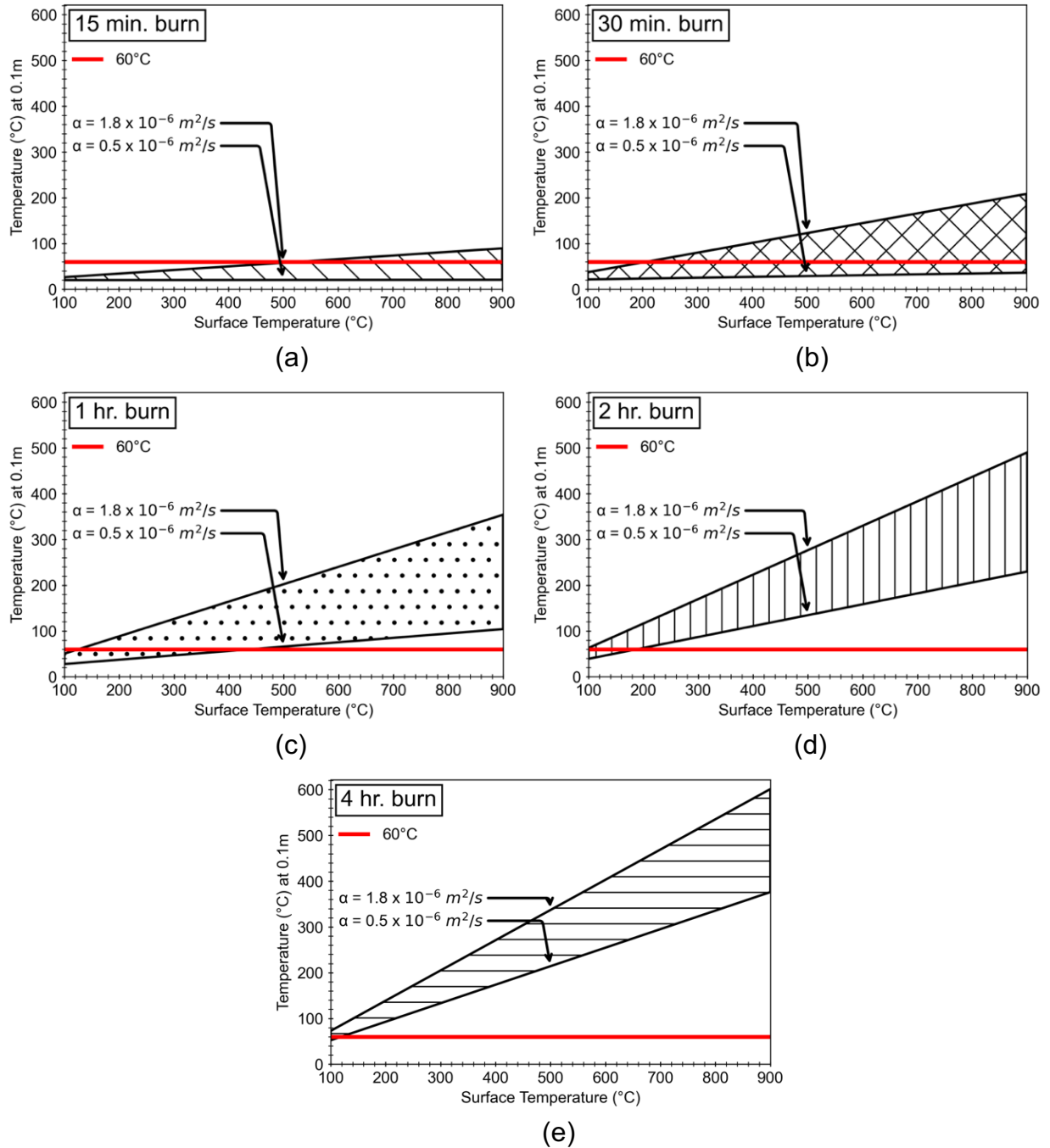


**Figure 4.** Soil temperature ( $^{\circ}\text{C}$ ) at 0.1m below the surface for a range of thermal diffusivities ( $0.5 \times 10^{-6} \leq \alpha \leq 1.8 \times 10^{-6} \text{ m}^2/\text{s}$ ) and constant surface temperatures ( $^{\circ}\text{C}$ ). (a) 15 minutes of burning, (b) 30 minutes of burning, (c) 1 hour of burning, (d) 2 hours of burning, and (e) 4 hours of burning

### Heat transfer results at 0.3m below the surface

The Uniform Plumbing Code (2021) requires water piping installation at a minimum of 0.305m below finished grade or 0.305m below the frost line. At the code compliant minimum burial depth, the 15 and 30-minute burn durations did not significantly increase soil temperatures above ambient temperature (20°C), and are not shown within this report.

For a one hour burn duration, thermal diffusivity of  $1.8 \times 10^{-6} \text{ m}^2/\text{s}$ , and ground surface temperature of 900°C, the maximum soil temperature at 0.3m below the ground surface was 27°C (Figure 5a), which is within operational temperatures for the pipelines (PPI 2009). The maximum operational temperature (60°C) of the pipelines is exceeded during a two-hour burn (Figure 5b) and a four-hour burn (Figure 5c) with sustained surface temperatures of 661°C and 233°C, respectively, and a soil thermal diffusivity of  $1.8 \times 10^{-6} \text{ m}^2/\text{s}$ .

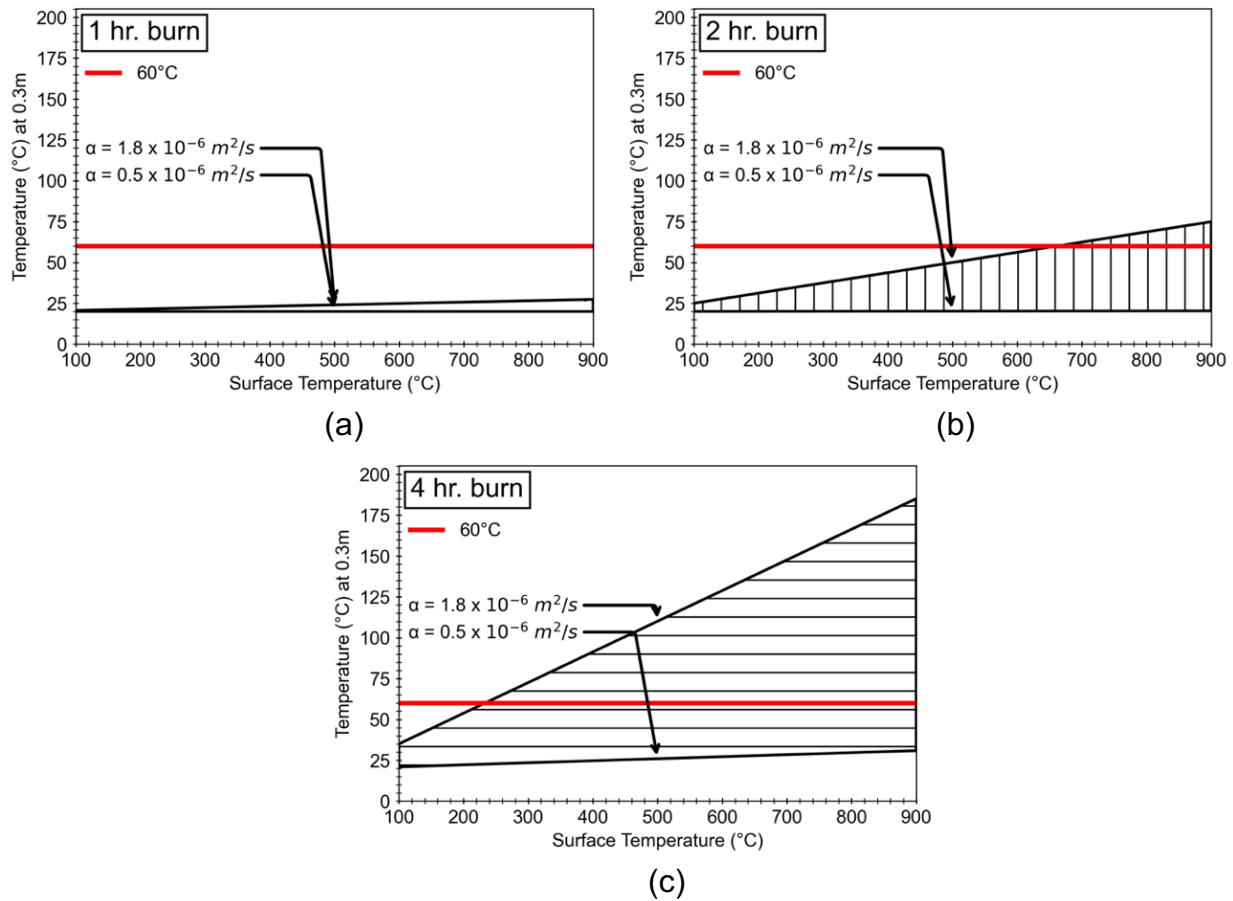


**Figure 5.** Soil temperature (°C) at 0.3m below the surface for a range of thermal diffusivities ( $0.5 \times 10^{-6} \leq \alpha \leq 1.8 \times 10^{-6} \text{ m}^2/\text{s}$ ) and constant surface temperatures (°C). (a) 1 hour of burning, (b) 2 hours of burning, and (c) 4 hours of burning

#### Heat transfer results at 0.46m below the surface

The 15-minute, 30-minute, and one-hour burn durations are not shown since they did not cause a noticeable increase in below ground soil temperature for any soil parameters analyzed at this depth. The industry recommended minimum burial depth for plastic pipes is 0.46m (MAB 2019). At this depth, the two-hour surface burn duration with a sustained surface temperature of 900°C and soil thermal diffusivity of  $1.8 \times 10^{-6} \text{ m}^2/\text{s}$  resulted in a maximum soil temperature of 24°C at 0.46m below the surface of the ground (Figure 6a).

At the same depth, the soil reached a maximum temperature of 58°C with four-hours of burn duration and the same sustained surface temperature and soil thermal diffusivity (Figure 6b). 58°C is just below the maximum operational temperatures of 60°C for the pipes considered.

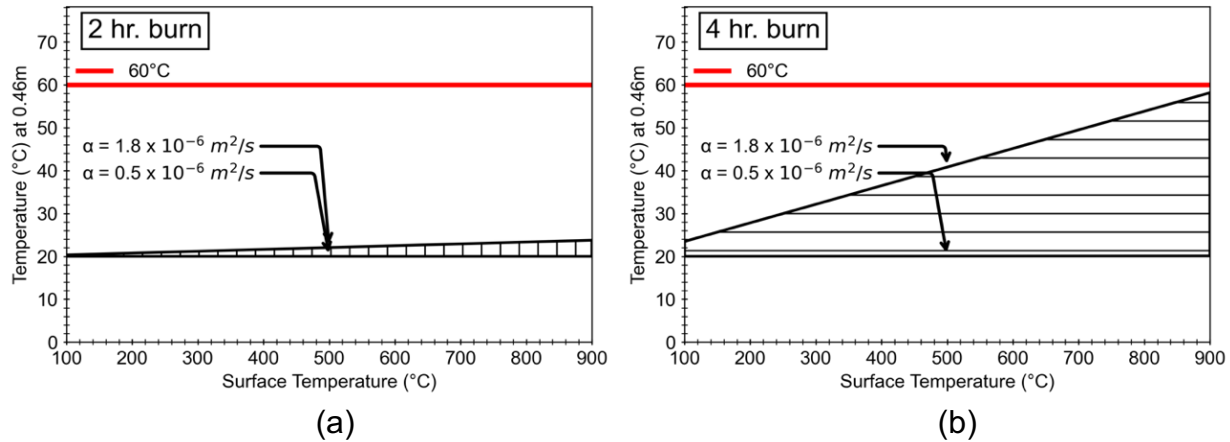


**Figure 6.** Soil temperature (°C) at 0.46m below the surface for a range of thermal diffusivities ( $0.5 \times 10^{-6} \leq \alpha \leq 1.8 \times 10^{-6} \text{ m}^2/\text{s}$ ) and constant surface temperatures (°C). (a) 2 hours of burning, and (b) 4 hours of burning

### Depth Below Ground

As discussed in the previous section, the temperature distribution through the soil can be quite large, since soil acts as a heat sink. Figure 7 shows a below ground soil temperature profile for a range of burn durations while holding thermal diffusivity constant at  $1.8 \times 10^{-6} \text{ m}^2/\text{s}$ . This thermal diffusivity is representative of a sandy loam soil and is the highest thermal diffusivity possible in a WUI community (Ochsner et al. 2001). Figure 7a shows the temperature distribution through the soil that is representative for a sustained surface temperature of 600°C for multiple burn durations. For a 15-minute burn duration, the maximum operational temperature of the pipes (60°C) was exceeded at 0.104m below

the surface. Whereas, a four-hour burn duration resulted in the maximum operational temperature of the pipes (60°C) exceeded at a maximum of 0.414m below the surface of the ground (Figure 7a). The upper bound surface temperatures expected from a fire in a WUI community is 900°C. When considering a 900°C sustained surface temperature for a 15-minute burn duration, the maximum operational temperature of the pipes (60°C) is exceeded at a maximum depth of 0.114m below the surface of the ground. For the four-hour, 900°C burn duration and temperature, maximum operational temperature of the pipes (60°C) was exceeded at a maximum depth of 0.455m below the ground surface.

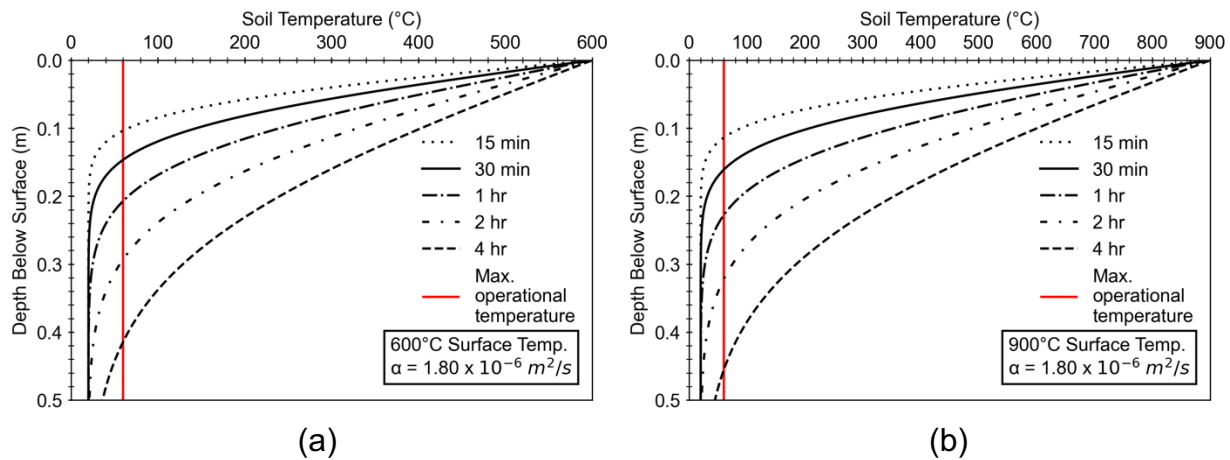


**Figure 7.** Soil temperature (°C) distribution to 0.5m below the surface with thermal diffusivity as ( $\alpha = 1.8 \times 10^{-6} \text{ m}^2/\text{s}$ ) for: (a) a representative structure fire (600°C), and (b) an upper bound structure fire (900°C)

Figure 8 presents the temperature distribution through the soil for a range of burn durations while holding thermal diffusivity constant at  $1.64 \times 10^{-6} \text{ m}^2/\text{s}$ . Thermal diffusivity of  $1.64 \times 10^{-6} \text{ m}^2/\text{s}$  (Soil Survey 2019) is representative of what could be found in a WUI community, such as Paradise, CA based on similar soil types reported (Bilskie 1994; DeVries 1963; Ochsner et al. 2001). Figure 8a shows the temperature distribution through the soil that could be representative for a sustained surface temperature of 600°C. A 15-

minute burn duration caused soil temperatures that exceeded maximum operational temperatures of the pipes at a depth of 0.099m below the ground surface. While a four-hour burn duration at a surface temperature of 600°C caused soil temperatures to exceed the maximum operational temperature of the pipes (60°C) at a maximum depth of 0.396m below the surface. A decrease in thermal diffusivity of  $0.16 \times 10^{-6} \text{ m}^2/\text{s}$  resulted in the maximum operational temperature of the pipes being exceeded five percent closer to the surface.

Figure 8b is a plot of thermal gradients through the soil when there is a sustained ground surface temperature of 900°C and a soil thermal diffusivity of  $1.64 \times 10^{-6} \text{ m}^2/\text{s}$ . The 15-minute burn duration caused soil temperatures to exceed the maximum operational temperature of the pipes (60°C) at a depth of 0.108m below the surface. Whereas for a four-hour burn duration the soil temperature exceeded the maximum operational temperatures of the pipes (60°C) at a depth of 0.435m below the surface. An increase in the sustained ground surface temperature from 600°C (Figure 8a) to 900°C (Figure 8b) resulted in the operational temperatures of the pipes being exceeded at a shallower depth from the surface of the ground (9%) for the both the 15-minute and four-hour burn durations.

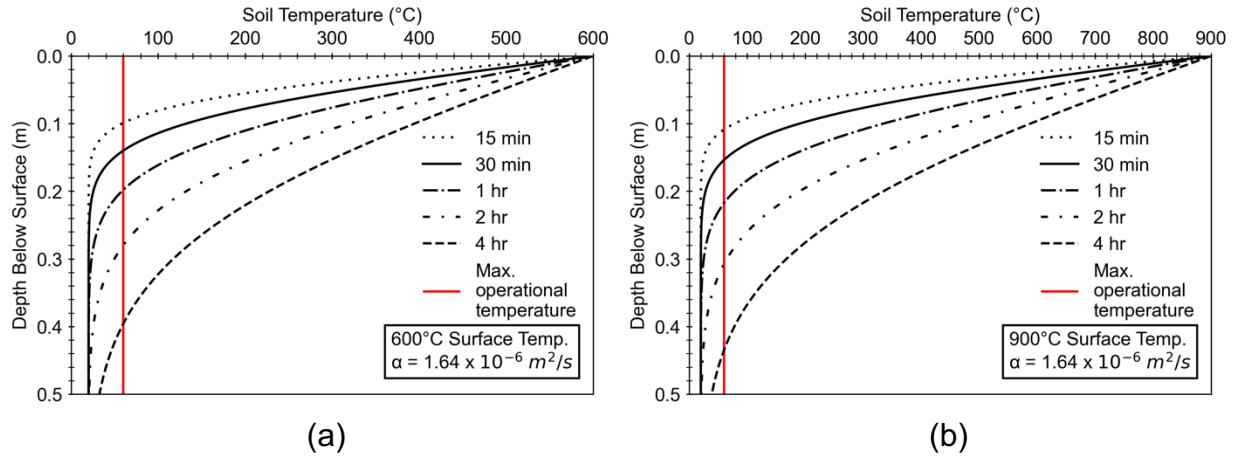


**Figure 8.** Soil temperature ( $^{\circ}\text{C}$ ) distribution to 0.5m below the surface with thermal diffusivity as ( $\alpha = 1.64 \times 10^{-6} \text{ m}^2/\text{s}$ ) for: (a) a representative structure fire ( $600^{\circ}\text{C}$ ), and (b) an upper bound structure fire ( $900^{\circ}\text{C}$ )

### Sensitivity Analysis

A sensitivity analysis was performed to investigate which parameters have the greatest impact on below ground soil temperatures. A base scenario (pipe burial depth, surface temperature, and soil thermal diffusivity) was chosen to represent a case where the maximum operational temperature of the pipes was exceeded. Depth below ground was set at 0.305m, the code minimum burial depth. A burn duration of two hours was selected as a median burn duration, while thermal diffusivity of  $1.64 \times 10^{-6} \text{ m}^2/\text{s}$  was selected as a value that is present in intermountain West WUI communities (Ochsner et al. 2001; Soil Survey 2019). A constant surface temperature of  $800^{\circ}\text{C}$  was selected to represent a potential ground surface temperature during a WUI fire (Schulze et al. 2020). Figure 9 is a tornado diagram that summarizes each variable in Equation 3 changing one at a time, while holding the remaining variables constant at the base case. The maximum and minimum values shown on Figure 9 represent the upper and lower bounds of potential scenarios in a WUI community.

Burial depth is observed to be the soil parameter that contributes the most to below ground soil temperatures. Decreasing the depth of the pipe from 0.305m to 0.1m resulted in an increase of soil temperature from 60°C to 427°C, while an increase in depth from 0.305m to 0.5m decreased the soil temperature from 60°C to 21°C. Burn duration is the second most influential parameter that effects the below ground soil temperature. This trend supports similar observations by Scotter (1970) who reported that it was the duration of increased surface temperatures that mattered more than the maximum temperature of the surface fire.

Increasing the burn duration from two-hours to four-hours increased the soil temperature by 86°C, while decreasing burn duration from two-hours to 15-minutes did not allow soil temperatures to increase above the ambient soil temperature of 20°C. Soil thermal diffusivity was set equal to  $1.64 \times 10^{-6} \text{ m}^2/\text{s}$  for the base case. An increase in thermal diffusivity to  $1.8 \times 10^{-6} \text{ m}^2/\text{s}$  resulted in soil temperatures increasing to 68°C at a soil depth of 0.305m. Decreasing thermal diffusivity to  $0.5 \times 10^{-6} \text{ m}^2/\text{s}$  only increased soil temperatures 0.3°C above the ambient soil temperature of 20°C at a soil depth of 0.305m. An increase in ground surface temperature to 900°C resulted in soil temperatures increasing to 65°C at a depth of 0.305m, but a decrease in surface burn temperature to 100°C decreased soil temperatures from 60°C to 24°C at a depth of 0.305m.

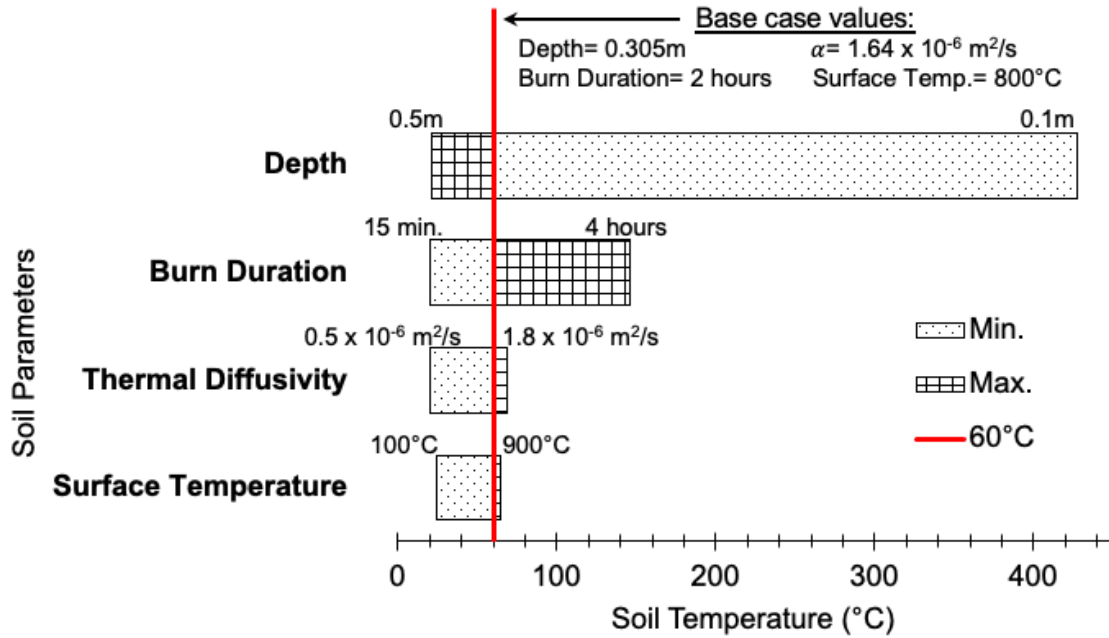


**Figure 9.** Tornado sensitivity plot of maximum and minimum soil parameters that contribute to below ground soil temperature that is representative of a WUI community.

### Fragility Function

A fragility function was developed to estimate the probability of exceeding the maximum operational temperature of the pipes (60°C) given varying burial depth. Maximum and minimum values for burial depth, burn duration, thermal diffusivity, and surface temperature were used as outlined in the sensitivity analysis. The fragility function follows the lognormal probability distribution function as given by Equation 7.

$$P(C|D = x) = \Phi\left(\frac{1}{\beta} \ln\left(\frac{x}{\theta}\right)\right) \quad [7]$$

$P(C|D = x)$  is the probability that a depth with  $D = x$  will cause soil temperatures to exceed 60°C.  $\Phi(\cdot)$  is the standard normal cumulative distribution function (CDF),  $\beta$  is the logarithmic standard deviation, and  $\theta$  is the median of the fragility function (depth with a

50% probability of exceeding 60°C). Thus, the development of the fragility function in Equation (7) is dependent on the estimation of the fragility parameters  $\beta$  and  $\theta$ .

The appropriate method for estimating the fragility function parameters,  $\beta$  and  $\theta$ , with this type of data is maximum likelihood estimation and follows the general form as outlined in Baker (2015):

$$\{\beta, \theta\} = \max_{\beta, \theta} \sum_{i=1}^m \left\{ \ln \binom{n_j}{z_j} + z_j \ln \Phi \left( \frac{\ln \frac{x_j}{\theta}}{\beta} \right) + (n_j - z_j) \ln \left( 1 - \Phi \left( \frac{\ln \frac{x_j}{\theta}}{\beta} \right) \right) \right\} \quad [8]$$

where  $m$  is the number of  $x_j$  depths considered, and  $z_j$  is the count of the number greater than 60°C out of the total  $n_j$  analyses. This summation was then maximized using software tools that produce the estimates of  $\beta$  and  $\theta$  that best fit the probabilities of exceedance for all burial depths.  $z_j$  was produced by solving Equation 3 over 50,000 unique times with different burn durations, thermal diffusivities, and surface temperatures.

The fragility curve was developed from the estimates of  $\beta$  and  $\theta$  from Equation 8 and resulted in the parameters,  $\beta = 0.5$  and  $\theta = 0.19$ . The fragility parameters are then used to solve Equation 7, providing the fragility curve shown in Figure 10.  $\theta = 0.19$  indicates that the depth where the probability of exceedance is 50% is at 0.19m below the surface. At the code minimum burial depth of 0.305m below the surface the probability of exceeding the 60°C maximum operational temperature of the pipes is 17%. At the industry recommend burial depth of 0.46m the probability of exceeding the 60°C maximum operational temperature of the pipes is 3.8%. At a depth of 0.1m that can commonly be associated with the junction between the structure and the pipeline the

probability of exceeding 60°C is 90%. This fragility function can be broadly implemented in WUI communities that fall within the soil and burn parameters of this report.

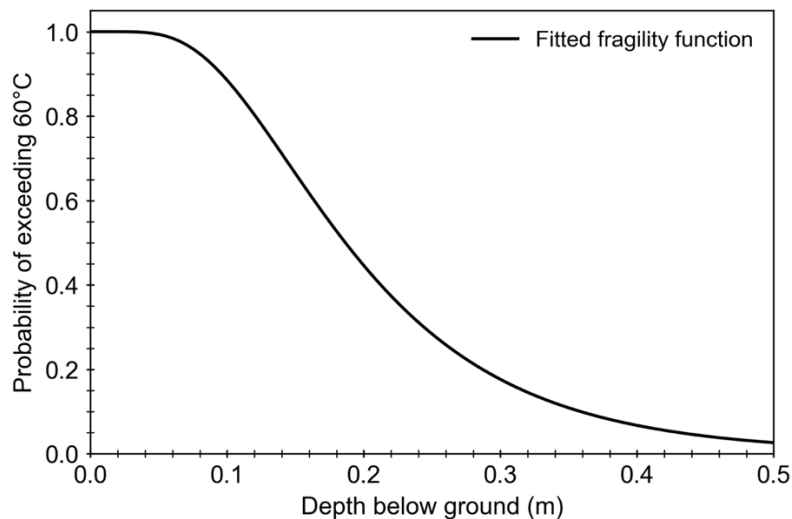


**Figure 10.** Fragility curve describing the probability of exceeding the maximum operational temperatures of buried pipes (60°C) based on burial depth (m).

## Limitations

There are certain inherent limitations that were built into this research, both with model choice and model inputs. A more comprehensive view of the temperature distribution through the soil profile would have been to incorporate all modes of heat transfer; radiative, convective, and conductive. However, for this research we considered heat transfer from wildfires as conduction only (Scotter 1970). Another limitation of the model used in this research is that it only considers constant surface temperature and constant surface heat flux. It is known that temperatures during a wildfire can vary significantly, and time temperature curves of such fires have been well documented. Modeling surface temperature as constant can both over and underestimate the true temperature of the soil underneath a wildfire. Variable temperatures within the wildfire also effect the burn

duration parameters of this research. After the wildfire has burned a significant portion of the available fuel; the wildfire will then begin to smolder at decreased temperatures. Smoldering is a period that can maintain elevated temperatures for hours to days depending on the conditions (Massman et al. 2008).

Soil properties such as moisture content and thermal diffusivity will change as the temperature of the soil is increased during a wildfire (Campbell et al. 1994; Smits et al. 2010). These changes to moisture content and thermal diffusivity with respect to time were not included in this research. The approach taken in Figures 4 – 6, where a broad range of thermal diffusivity values were considered, helps to reduce the impacts of these time dependent changes. This is a simplification of the overall behavior of both the soil properties and the temperature of the soil underneath a wildfire but provides a baseline of general trends that could be present in WUI communities.

## **Conclusions and Future Work**

Wildfires in WUI communities have increased in frequency over the last several decades and are expected to continue to increase in both frequency and intensity in the years to come due to the ongoing effects of climate change. Wildfires are not only destroying above ground infrastructure, but can damage buried utilities that have, until recently, been considered to be unaffected. The water contamination crises in the towns of Santa Rosa and Paradise were a direct result of the wildfires that burned through those communities. Several key soil parameters commonly found in WUI communities were analyzed using established mathematical models (Carslaw and Jaeger 1959). Using operational temperatures of buried utilities as a focus, we can conclude that burial depth and surface

burn duration play a key role in determining if the maximum operational temperature of the buried utility will be exceeded.

At the code minimum burial depths of 0.305m below the frost line and industry recommended burial depths of 0.46m below the frost line, changes in below ground soil temperature are highly sensitive to variations in depth and burn duration. Under maximum conditions tested, a change in depth of one centimeter from 0.46m to 0.45m is all that is required to exceed the maximum operational temperature of the buried pipe (Figure 7b). Such a small tolerance for variability is problematic considering that installation methods can have tolerances well in excess of one centimeter, providing no margin of safety against exposure to temperatures that are too high. The connection point of the service lateral to the house can be much closer to the surface, exposing the pipes to extreme temperatures well above the maximum operational temperatures (Figure 4). Exposure to extreme temperatures can occur by conduction through soil, the foundation of the house, or through direct flame contact if the service laterals are only separated by combustible materials.

Further research is needed to investigate the effects of exceeding the maximum operational temperature of the service lateral distribution system. Visual evidence of melted pipe material can indicate that the pipe in question has been damaged and could potentially have leached previously inert chemicals into the water system. However, if no visual cues are present, it is impossible to determine if the operational temperature of the pipe has been exceeded, and if any contaminants have been transferred into the water.

Lastly, it is important to understand the duration of time that pipes can be above their operational temperatures before contaminants are transferred into the water.

## **Appendix**

### Heat transfer results at 0.2m below the surface

Figure A-1 shows the soil temperatures at 0.2m below the surface for a range of surface burn durations, thermal diffusivities, and surface temperatures. The 15-minute burn duration is not shown, since it did not cause a noticeable increase in below ground soil temperature for any range of surface temperatures or thermal diffusivities analyzed at 0.2m below the surface. Figure A-1a shows that 30 minutes of sustained surface temperatures of 900°C with maximum thermal diffusivity only raised the below ground soil temperature to 31.4°C, which does not exceed the maximum operational temperatures of the pipelines (60°C). The maximum operational temperature (60°C) of the pipelines is exceeded during a one-hour burn (Figure A-1b) and a two-hour burn (Figure A-1c) with sustained surface temperatures of 527°C and 207°C respectively, and a thermal diffusivity of  $1.8 \times 10^{-6} \text{ m}^2/\text{s}$ . Figure A-1d shows that for the four-hour surface burn, maximum operational temperatures of the pipes are exceeded with a constant surface temperature of 125°C and a thermal diffusivity of  $1.8 \times 10^{-6} \text{ m}^2/\text{s}$ , or a constant surface temperature of 438°C and a thermal diffusivity of  $0.5 \times 10^{-6} \text{ m}^2/\text{s}$ .

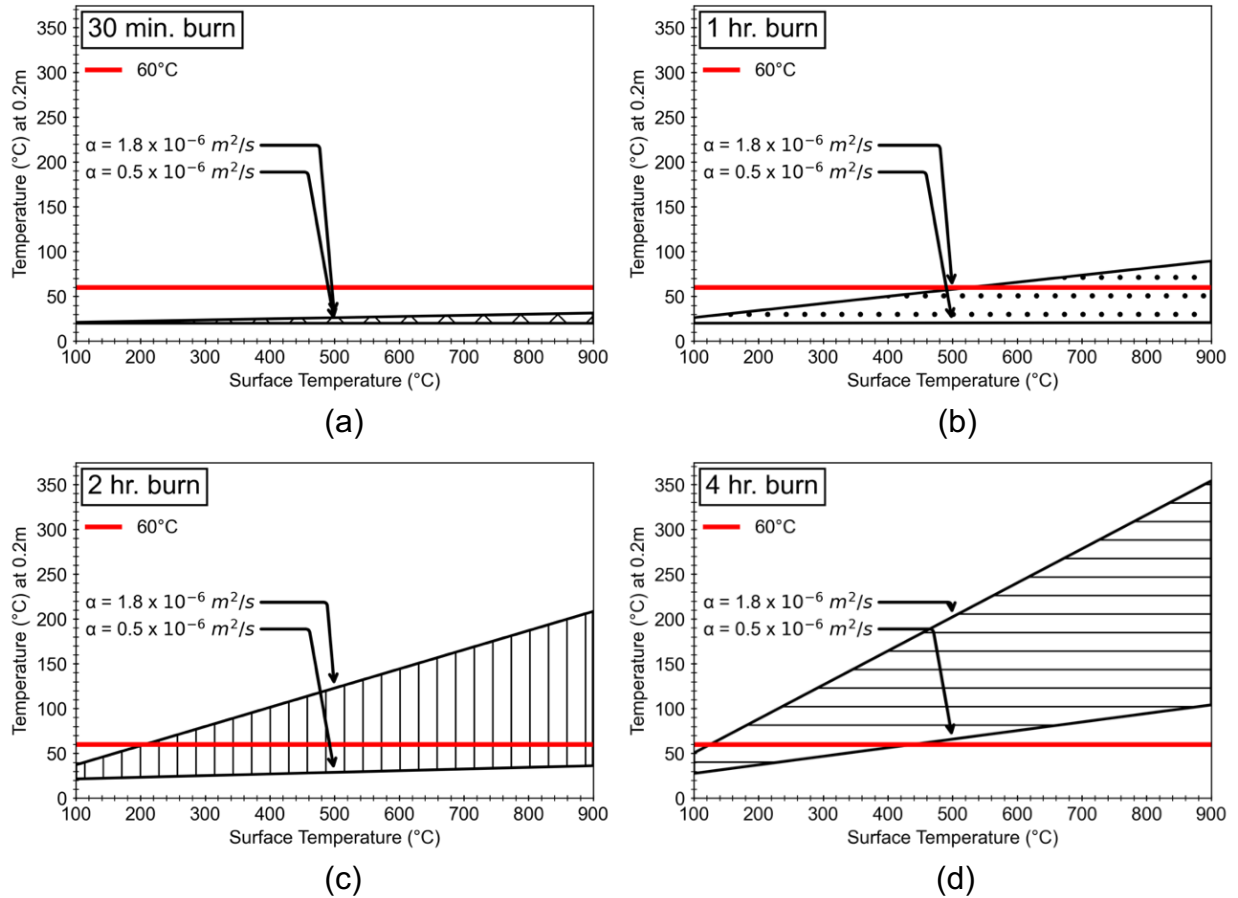


**Figure A-1.** Soil temperature (°C) at 0.2m below the surface for a range of thermal diffusivities ( $0.5 \times 10^{-6} \leq \alpha \leq 1.8 \times 10^{-6} \text{ m}^2/\text{s}$ ) and constant surface temperatures (°C). (a) 30 minutes of burning, (b) 1 hour of burning, (c) 2 hours of burning, and (d) 4 hours of burning

Heat transfer results at 0.4m below the surface

Figure A-2 shows the results of the analysis at 0.4m below the surface for a range of surface temperatures, thermal diffusivities, and burn durations. At 0.4m below the surface burn durations of 15-minutes, 30-minutes, and one-hour did not significantly increase soil temperatures above the ambient temperature of 20°C and are not included in this report. Figure A-2a shows that although the two-hour burn duration did increase soil temperatures at a depth of 0.4m, temperatures were only able to reach 31°C with a 900°C

constant surface temperature and a thermal diffusivity of  $1.8 \times 10^{-6} \text{ m}^2/\text{s}$ . The maximum operational temperatures of the pipelines ( $60^\circ\text{C}$ ) is exceeded at four hours (Figure A-2b) with a constant surface temperature of  $527^\circ\text{C}$  with a thermal diffusivity of  $1.8 \times 10^{-6} \text{ m}^2/\text{s}$ . The maximum soil temperature at 0.4m below ground that was achieved at the upper limit of these analyses is  $89^\circ\text{C}$ .

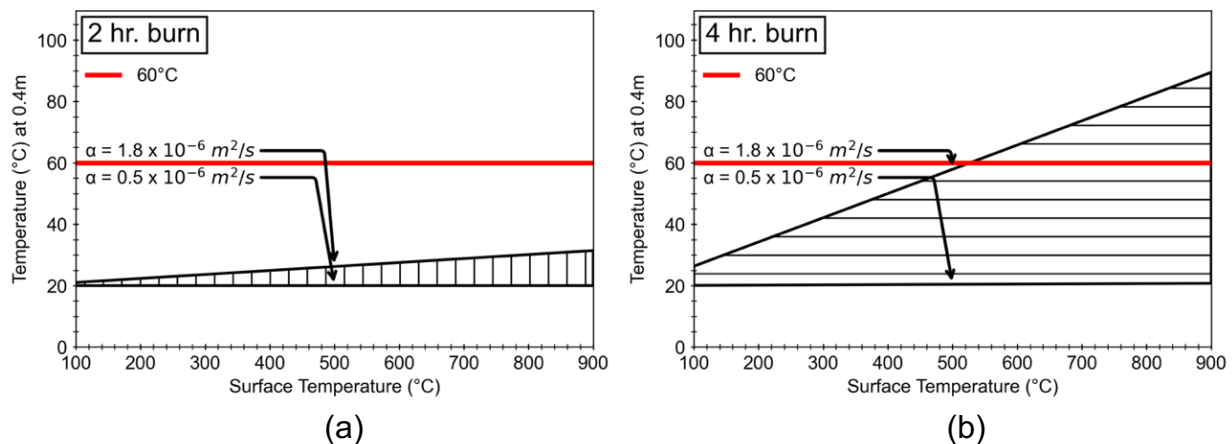


**Figure A-2.** Soil temperature ( $^\circ\text{C}$ ) at 0.4m below the surface for a range of thermal diffusivities ( $0.5 \times 10^{-6} \leq \alpha \leq 1.8 \times 10^{-6} \text{ m}^2/\text{s}$ ) and constant surface temperatures ( $^\circ\text{C}$ ). (a) 2 hours of burning, and (b) 4 hours of burning

### Heat transfer results at 0.5m below the surface

Figure A-3 shows the soil temperatures at a depth of 0.5m below the surface for a range of surface burn durations, thermal diffusivities, and surface burn temperatures. The 15-minute, 30-minute, and one-hour burn durations are not shown since they did not cause a noticeable increase in below ground soil temperature for any range of surface temperatures or thermal diffusivities tested at 0.5m below the surface. The two and four-hour burn durations caused a noticeable increase in soil temperatures at 0.5m below the surface, however neither the two-hour nor the four-hour burn times exceeded the

maximum operational temperature (60°C) of the service lateral pipes at that depth. The two-hour burn increased soil temperatures to 22°C (Figure A-3a), while the four-hour burn increased soil temperatures to 45°C (Figure A-3b) under the maximum temperatures and thermal diffusivities considered (900°C and  $1.8 \times 10^{-6} \text{ m}^2/\text{s}$  respectively).

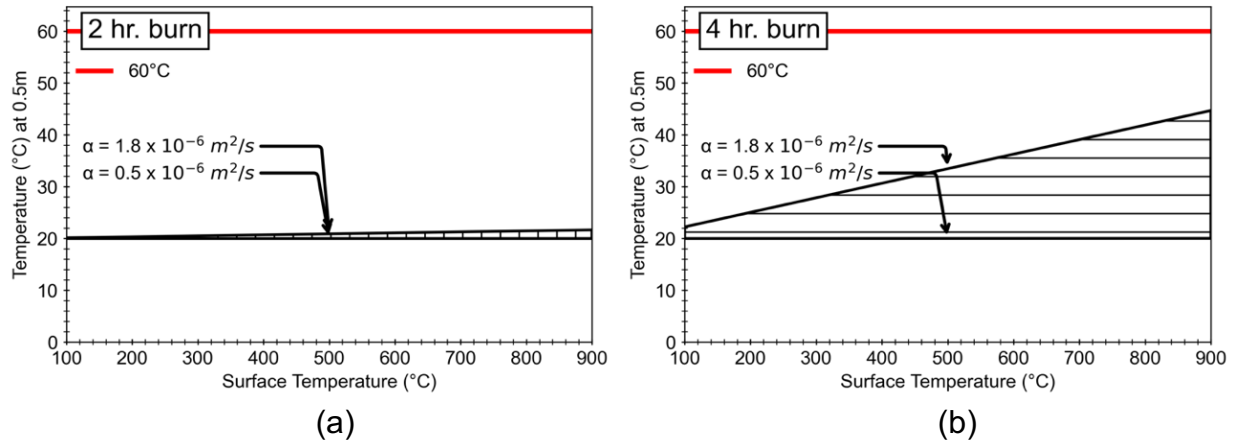


**Figure A-3.** Soil temperature (°C) at 0.5m below the surface for a range of thermal diffusivities ( $0.5 \times 10^{-6} \leq \alpha \leq 1.8 \times 10^{-6} \text{ m}^2/\text{s}$ ) and constant surface temperatures (°C). (a) 2 hours of burning, and (b) 4 hours of burning

## References

- Abu-Hamdeh, N.H. 2003. Thermal properties of soils as affected by density and water content. *Biosystems Engineering* 86 (1): 97 – 102. [https://doi.org/10.1016/S1537-5110\(03\)00112-0](https://doi.org/10.1016/S1537-5110(03)00112-0)
- Abu-Hamdeh, N.H., and Reeder, R.C. 2000. Soil thermal conductivity: Effects of density, moisture, salt concentration, and organic matter. *Soil Science Society of America Journal* 64: 1285 – 1290. <https://doi.org/10.2136/sssaj2000.6441285x>
- American Water Works Association. 2006. PE pipe – design and installation. AWWA Manual M55. American Water Works Association.
- Baker, J. 2015. Efficient analytical fragility function fitting using dynamic structural analysis. *Earthquake Spectra*, 31 (1): 579 – 599. <https://doi.org/10.1193/021113EQS025M>
- Beitel, J., and Iwankiw, N. 2008. Analysis of needs and existing capabilities for full-scale fire resistance testing. National Institutes of Standards and Technology, Gaithersburg, MD.
- Bilskie, J.R. 1994. Dual probe methods for determining soil thermal properties: Numerical and laboratory study. Ph.D. Dissertation. Iowa State University.
- Cal Fire. 2018. Wildfire activity statistics. California Department of Forestry and Fire Protection.
- Cal Fire (a). 2020. Top 20 most destructive California wildfires. [https://www.fire.ca.gov/media/t1rdhizr/top20\\_destruction.pdf](https://www.fire.ca.gov/media/t1rdhizr/top20_destruction.pdf) (accessed 03/28/2021)
- Cal Fire (b). 2020. 2020 Fire Siege. Report prepared by: George Morris III and Carrie Dennis.
- Campbell, G.S., Jungbauer Jr, J.D., Bidlake, W.R., Hungerford, R.D. 1994. Predicting the effect of temperature on soil thermal conductivity. *Soil Science* 158 (5): 307 – 313. <https://doi.org/10.1097/00010694-199411000-00001>
- Carslaw, H.C., and Jaeger, J.C. 1959. Conduction of heat in soils. 2<sup>nd</sup> Edition. Oxford University Press London.
- Chong, N.S., Abdulramoni, S., Patterson, D., and Brown, H. 2019. Releases of fire-derived contaminants from polymer pipes made of polyvinyl chloride. *Toxics* 7 (4): 1 – 14. <https://doi.org/10.3390/toxics7040057>

- City of Santa Rosa Water. 2018. Post-fire water quality investigation: Analysis of cause of water contamination. Technical memorandum 1. City of Santa Rosa Government: Santa Rosa CA.
- Copper Development Association. 2010. The copper tube handbook. Copper Development Association Inc, New York, NY.
- DeVries D.A. 1963. Thermal Properties of Soils. In W.R. van Wijk (ed.) Physics of Plant Environment. North-Holland Publishing Company, Amsterdam.
- Drysdale, D. 2011. An introduction to fire dynamics 3<sup>rd</sup> edition. John Wiley and Sons. New York, NY.
- Duffy, D.P. 2019. The perfect pipe. Water World.  
<https://www.waterworld.com/home/article/14071043/the-perfect-pipe#:~:text=The%20most%20common%20pipe%20diameter,diameter%20up%20to%206%20inches>. (accessed 5/12/21)
- Duran, B.A. 2013. Galvanized steels performance in extreme temperatures. American Galvanizers Association.  
<https://galvanizeit.org/knowledgebase/article/galvanized-steel-s-performance-in-extreme-temperatures>. (accessed 2/15/21)
- Georg Fischer. 2010. Schedule 80 PVC and CPVC, schedule 40 PVC piping systems technical manual. Georg Fischer Piping systems, Tustin, CA.
- Home Innovation Research Labs. 2013. Design guide residential PEX water supply plumbing systems, 2<sup>nd</sup> Edition. Prepared for Plastic Pipe Institute, Irving, TX.
- Insurance Information Institute. 2021. Facts + statistics: Wildfires.  
<https://www.iii.org/fact-statistic/facts-statistics-wildfires> (accessed 05/10/21)
- Isaacson, K.P., Proctor, C.R., Wang, Q.E., Edwards, E.Y., Noh, Y., Shah, A.D., and Whelton, A.J. 2021. Drinking water contamination from the thermal degradation of plastics: implications for wildfire and structure fire response. Environmental Science Water Research and Technology 7: 274 – 284.  
<https://doi.org/10.1039/D0EW00836B>
- Kasler, D. 2017. Wine country wildfires costs now top \$9 billion, costliest in California's history. The Sacramento Bee.  
<https://www.sacbee.com/news/california/fires/article188377854.html> (accessed 5/15/21)
- Kim, A.K., and Lougheed, G.D. 1990. The protection of glazing systems with dedicated sprinklers. Journal of Fire Protection Engineering 2(2): 49 – 59.  
<https://doi.org/10.1177/104239159000200202>

- Márquez, J.M.A., Bohórquez, M.A.M., and Melgar, S.G. 2016. Ground thermal diffusivity calculation by direct soil temperature measurement. Application to very low enthalpy geothermal energy systems. *Sensors* 16 (3): 306.  
<https://doi.org/10.3390/s16030306>
- Massman, W.J., Frank, J.M., Reisch, N.B. 2008. Long-term impacts of prescribed burns on soil thermal conductivity and soil heating at a Colorado Rocky Mountain site: a data/model fusion study. *International Journal of Wildland Fire* 17: 131 – 146.  
<https://doi.org/10.1071/WF06118>
- Massman, W.J., Frank, J.M., Shepperd, W.D., and Platten, M.J. 2003. In situ soil temperature and heat flux measurements during controlled surface burns at a Southern Colorado forest site. *USDA Forest Service Proceedings RMRS-P-29*: 69 – 88.
- Municipal Advisory Board. 2020. MAB model specifications for PE 4710 buried potable water service, distribution and transmission pipes and fittings. Plastic Pipe Institute, Irving, TX.
- Löw, P. 2019. The natural disasters of 2018 in figures – Losses in 2018 dominated by wildfires and tropical storms. Munich Re Group.  
<https://www.munichre.com/topics-online/en/climate-change-and-natural-disasters/natural-disasters/the-natural-disasters-of-2018-in-figures.html>  
(accessed 5/15/21)
- Paradise Irrigation District. Water system recovery plan. Paradise Irrigation District: Paradise, CA, 2019.
- Plastic Pipe Institute. 2009. Frequently asked questions: HDPE pipe for water distribution and transmission applications. Plastic Pipe Institute, Irving, TX.
- Proctor, C.R., Lee, J., Yu, D., Shah, A.D., and Whelton, A.J. 2020. Wildfire caused widespread drinking water distribution network contamination. *AWWA Water Science*: 1 – 14. <https://doi.org/10.1002/aws2.1183>
- Ochsner, T.E., Horton, R., and Ren, T. 2001. A new perspective on soil thermal properties. *Soil Science Society of America Journal* 65: 1641 – 1647.  
<https://doi.org/10.2136/sssaj2001.1641>
- Quarles, S.L., and Sindelar, M. 2011. Wildfire ignition resistant home design (WIRHD) program: Full-scale testing and demonstration final report. United States.  
<https://doi.org/10.2172/1032503>
- Radeloff, V.C., Helmers, D.P., Kramer, H.A., Mockrin, M.H., Alexandre, P.M., Bar-Massada, A., Batusic, V., Hawbaker, T.J., Martinuzzi, S., Syphard, A.D., Stewart, S.I. 2018. Rapid growth of the US wildland-urban interface raises wildfire risk. *Proc. National Academy of Sciences U.S.A.* 115(13): 3314 – 3319.  
<https://doi.org/10.1073/pnas.1718850115>

- Rehm, R.G., Hamins, A., Baum, H.R., McGrattan, K.B., and Evans, D.D. 2002. Community-scale fire spread. Proceedings of California's 2001 Wildfire Conference: 10 years after the 1991 East Bay Hills Fire.
- Schulze, S.S., and Fischer, E.C. 2021. Prediction of water distribution system contamination based on wildfire burn severity in wildland urban interface communities. ACS ES&T 1(2): 291 – 299.  
<https://doi.org/10.1021/acsestwater.0c00073>
- Schulze, S.S., Fischer, E.C., Hamideh, S., and Mahmoud, H. 2020. Wildfire impacts on schools and hospitals following the 2018 California Camp Fire. Natural Hazards 104: 901 – 925. <https://doi.org/10.1007/s11069-020-04197-0>
- Scotter, D.R. 1970. Soil temperatures under grass fires. Australian Journal of Soil Research 8: 273 – 279. <https://doi.org/10.1071/SR9700273>
- Sharpe, I.P. and Associates. 2010. Underground water service lines: Material usage trends 1965 – 2009. Irwin P. Sharpe and Associates, Westfield NJ.
- Silvani X., and Morandini, F. 2009. Fire spread experiments in the field: Temperature and heat fluxes measurements. Fire Safety Journal 44: 279 – 285.  
<https://doi.org/10.1016/j.firesaf.2008.06.004>
- Smits, K.M., Kirby, E., Massman, W.J., Baggett, L.S. 2016. Experimental and modeling study of forest fire effect on soil thermal conductivity. Pedosphere 26(4): 462 – 473. [https://doi.org/10.1016/S1002-0160\(15\)60057-1](https://doi.org/10.1016/S1002-0160(15)60057-1)
- Soil Survey Staff. 2019. Web Soil Survey. Natural Resources Conservation Service, United States Department of Agriculture.  
<https://websoilsurvey.sc.egov.usda.gov/App/HomePage.htm> (accessed 02/10/2021).
- Uniform Plumbing Code. 2021. 609.1 Installation. International Association of Plumbing and Mechanical Officials Ontario, CA.
- Van Rossum, G. 2020. The Python Library Reference, release 3.8.3, Python Software Foundation.
- Wells, C.G., Campbell, R.E., DeBano, L.F., Lewis, C.E., Fredriksen, R.L., Franklin, E.C., Froelich, R.C., and Dunn, P.H. 1979. Effects of fire on the soil: a state-of-the-knowledge review. USDA Forest Service General Technical Report WO-7.